Acta Crystallographica Section C
Crystal Structure Communications
ISSN 0108-2701

A low-temperature polymorph of *m*-quinquephenyl

Ligia R. Gomes,[a] R. Alan Howie,[b] John Nicolson Low,[b]* Ana S. M. C. Rodrigues[c] and Luís M. N. B. F. Santos[c]

[a]REQUIMTE, Departamento de Química e Bioquímica, Faculdade de Ciências, Universidade do Porto, Rua do Campo Alegre 687, P-4169 007 Porto, Portugal, [b]Department of Chemistry, University of Aberdeen, Meston Walk, Old Aberdeen AB24 3UE, Scotland, and [c]Centro de Investigação em Química, Departamento de Química e Bioquímica, Faculdade de Ciências, Universidade do Porto, Rua do Campo Alegre 687, P-4169 007 Porto, Portugal
Correspondence e-mail: jnlow111@gmail.com

Received 31 October 2012
Accepted 9 November 2012
Online 13 November 2012

A low-temperature polymorph of 1,1′:3′,1′′:3′′,1′′′:3′′′,1′′′′-quinquephenyl (*m*-quinquephenyl), $C_{30}H_{22}$, crystallizes in the space group $P2_1/c$ with two molecules in the asymmetric unit. The crystal is a three-component nonmerohedral twin. A previously reported room-temperature polymorph [Rabideau, Sygula, Dhar & Fronczek (1993). *Chem. Commun.* pp. 1795–1797] also crystallizes with two molecules in the asymmetric unit in the space group $P\overline{1}$. The unit-cell volume for the low-temperature polymorph is 4120.5 (4) Å^3, almost twice that of the room-temperature polymorph which is 2102.3 (6) Å^3. The molecules in both structures adopt a U-shaped conformation with similar geometric parameters. The structural packing is similar in both compounds, with the molecules lying in layers which stack perpendicular to the longest unit-cell axis. The molecules pack alternately in the layers and in the stacked columns. In both polymorphs, the only interactions between the molecules which can stabilize the packing are very weak C—H$\cdots\pi$ interactions.

Comment

Polyphenyls are used in technological industries, either directly (*e.g.* as dyes, thermal printing materials or coolants) or as starting materials for functionalized derivatives that are incorporated in, for instance, nonspreading lubricants, emulsifiers, optical brighteners, crop protection products and plastics. In spite of this, experimental data for the thermochemical parameters of these compounds that would permit inferences to be made concerning not only their relative stability, but also structure/molecular energetics relationships or thermophysical properties, are scarce.

In the course of a thermochemical study of polyphenylenes, particularly with regard to the effect of isomerization on the fusion temperatures, heat capacities, enthalpies of formation and enthalpies of vaporization, *m*-quinquephenyl, (I), has been synthesized, following a similar procedure to that used for a previously optimized Suzuki–Miyaura cross-coupling reaction (Suzuki, 2011; Miyaura, 2002) for polyphenyl compounds (Lima *et al.*, 2011). A search of the literature revealed that (I) had already been structurally characterized by X-ray diffraction at room temperature (283–303 K; Rabideau *et al.*, 1993). Nevertheless, it is well known that isomers belonging to the parent series of *p*-polyphenyl oligomers [*n*(phenyl) = 3–4] undergo solid-phase transitions (Baker *et al.*, 1990, and references therein). Those transitions are characterized by an order/disorder phase change, from twisted (at lower temperatures) to planar (when heated) (Delugeard *et al.*, 1976; Baudour *et al.*, 1978), so the question of whether a phase transition would occur in the *m*-quinquephenyl isomer was raised, driving interest in the structural characterization of the compound at low temperatures. Furthermore, the identification and characterization of the polymorphic forms is essential to an accurate interpretation of, for instance, experimental calorimetric results.

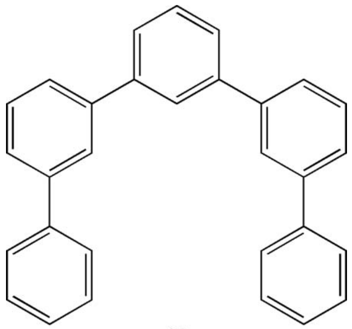

(I)

The low-temperature (LT) measurement, performed at 150 K, revealed that (I) crystallizes in the space group $P2_1/c$ with a unit-cell volume of 4120.5 (4) Å^3, and with two molecules (LT*A* and LT*B*) in the asymmetric unit (Fig. 1). These data show that the structure at low temperature is a polymorph of the earlier structure of (I) found by Rabideau *et al.* (1993) in a room-temperature (RT) determination ($R = 0.052$). At RT, (I) crystallizes in the space group $P\overline{1}$ with a unit-cell volume of 2102.3 (6) Å^3, and with two molecules in the asymmetric unit (RT*A* and RT*B*; Fig. 2). The RT unit-cell dimensions are: a = 7.7620 (6), b = 13.618 (2) and c = 21.623 (5) Å, and α = 80.58 (2), β = 85.26 (1) and γ = 89.71 (1)°. As can be seen from the crystal data table for the LT structure, there is a rough relationship between the unit-cell dimensions for each compound: $a'(\mathrm{RT}) \simeq b(\mathrm{LT})$, $b' \simeq a$, $c' \simeq c/2$, $\alpha' \simeq (180 - \beta)°$, and β' and γ' are quite close to 90°, so swapping the a and b axes and doubling c effectively changes the RT cell to the LT cell.

The *m*-polyphenyls might be expected to adopt a zigzag conformation in order to minimize steric repulsion between the phenyl groups, but in both the LT and RT crystal structures of (I) the U-shaped conformation is preferred. Theoretical calculations made earlier using MM2/87 (Rabideau *et al.*, 1993) showed that there is no apparent energetic restraint preventing the zigzag conformation in favour of the U-shaped

doi:10.1107/S0108270112046392

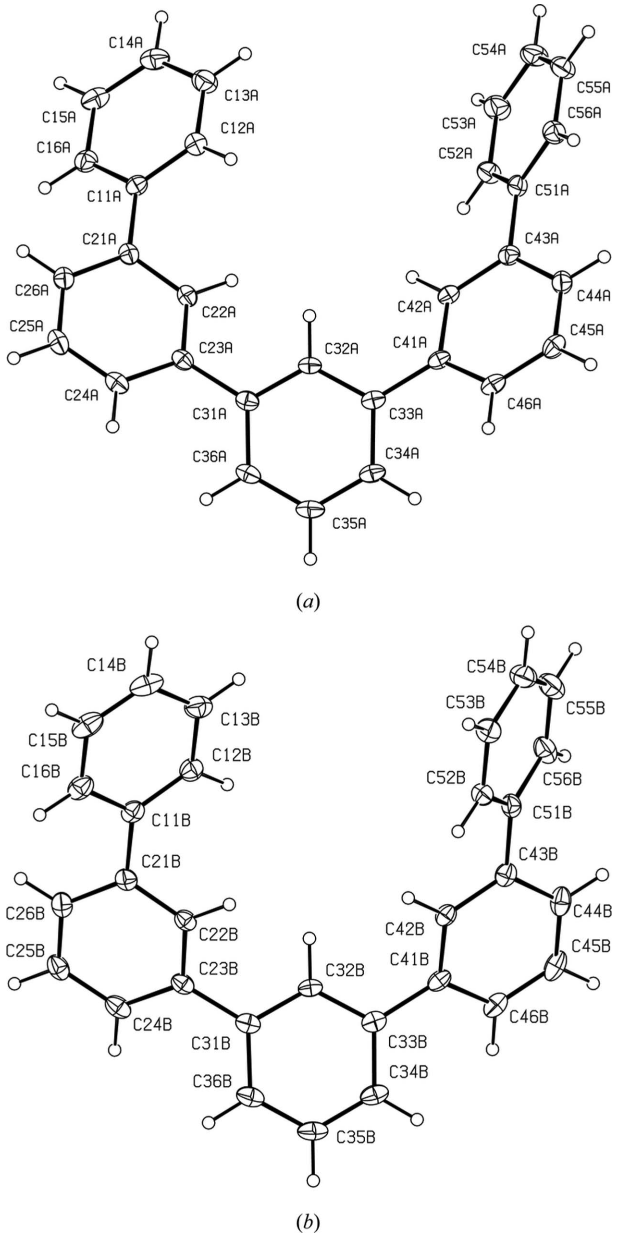

Figure 1
Molecules (*a*) LT*A* and (*b*) LT*B* of (I), showing the atom-numbering scheme. Displacement ellipsoids are drawn at the 30% probability level.

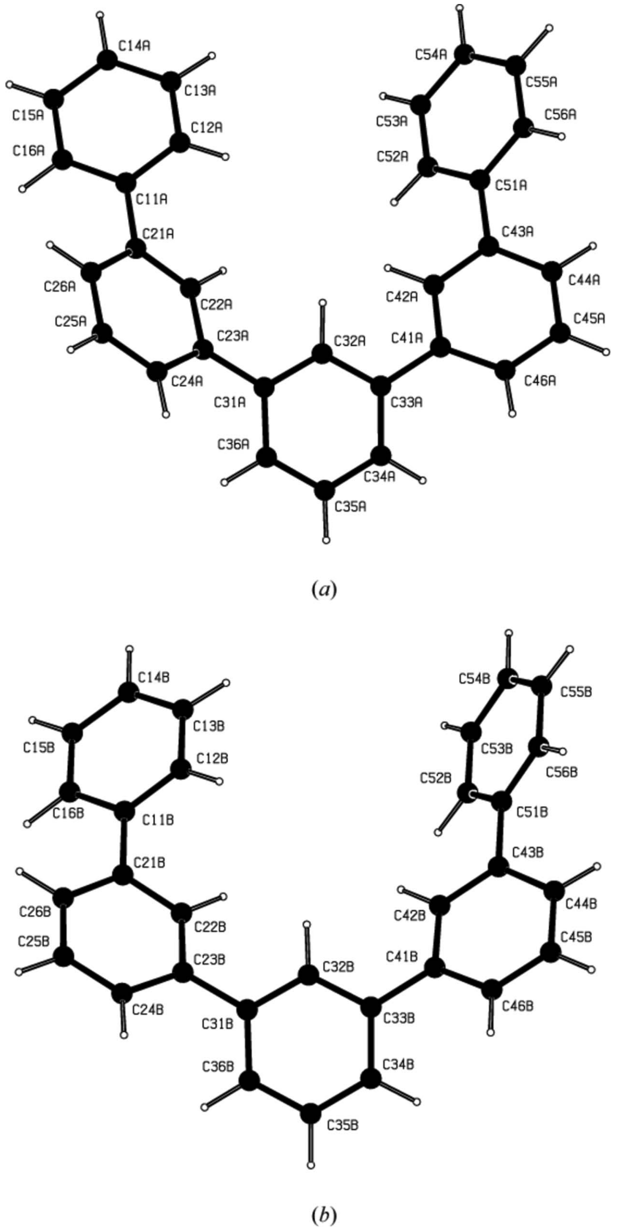

Figure 2
Molecules (*a*) RT*A* and (*b*) RT*B* of (I), taken from Rabideau *et al.* (1993), showing the atom-numbering scheme. The spheres are of arbitrary size.

conformation. The calculations were indicative that both conformers and their intermediate geometries are energetically similar, with torsion barriers of about 5 kJ mol^{-1}. All molecules have a very similar geometry. The dihedral angles between successive rings along the chain (Table 1) show that they lie within the same angular range and show similar trends. The results of a least-squares fit of the 30 C atoms using *PLATON* MOLFIT with quaternion transformation (Mackay, 1984; Spek, 2009) for the molecules in pairs are given in Table 2. Columns 3 and 5 provide values for the root-mean-square (r.m.s.) distance between equivalent (overlapping/superimposed) atoms in the fitted molecules. These give rise to values for the molecular isometricity index, defined as $I_i(n^*) = |[\Sigma(\Delta R_i)^2/n]^{1/2} - 1| \times 100$ for $n = 30$ (Kálmán *et al.*, 1993), given in columns 4 and 6 of Table 2. The r.m.s. bond-length and bond-angle differences between equivalent bonds and angles within each pair of molecules are also given in Table 2. As a consequence of the arbitrary choice of asymmetric unit, molecules *A* and *B* are mirror images of one another, as shown by the need to invert one of them to optimize the fit with the other. The MOLFIT parameters and the dihedral angles are indicative that the molecules have very similar conformations, as can be best viewed in the plots of the fitted molecules given in Fig. 3.

The values in Table 3 are consistent with the molecules in each bimolecular asymmetric unit being related to one another by a noncrystallographic glide plane, which ensures the invariance of the *z* coordinates for each pair of molecules; for the RT structure it is an *a*-glide parallel to (010), while for

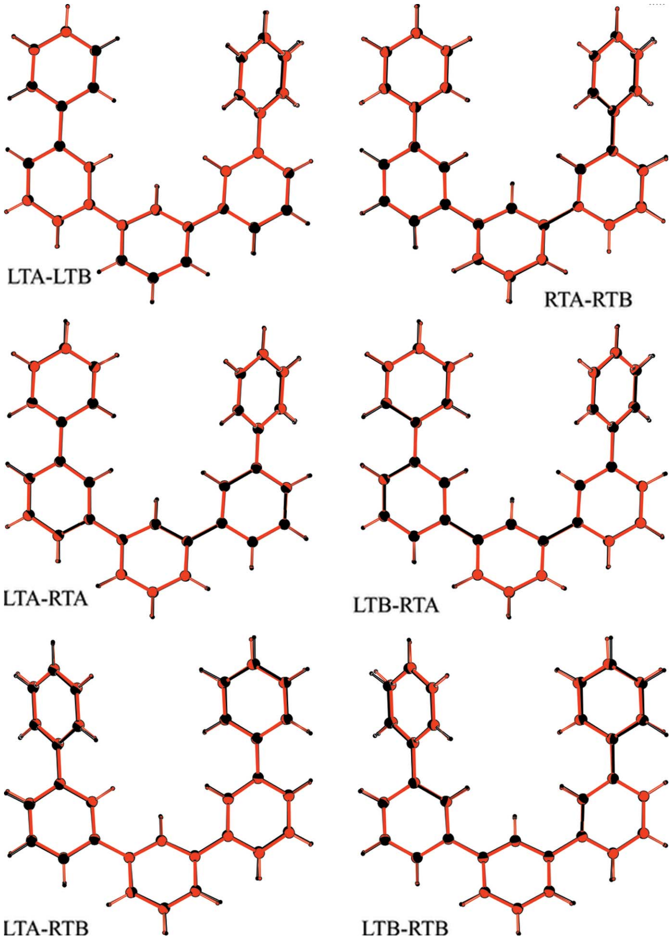

Figure 3
Molecular overlay diagrams for all six possible combinations of the molecules of the two structures. Black denotes the RT structure and lighter shading the LT one.

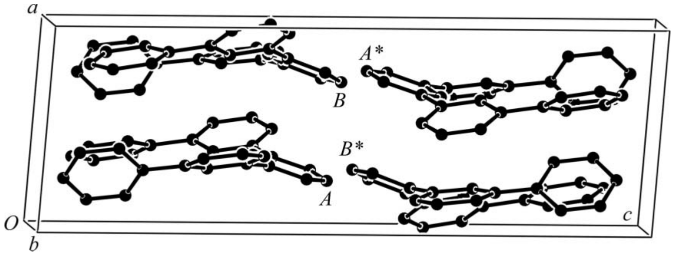

Figure 5
A view of the packing of the molecules in the unit cell of the RT form of (I), viewed along the *b* axis. H atoms have been omitted for clarity. Molecules labelled with an asterisk (*) are at the symmetry position $(-x + 1, -y + 1, -z + 1)$.

the LT structure it is a *b*-glide parallel to (100). Thus, in both structures, the molecules in the asymmetric unit sit above one another, with a fractional separation of 0.5 along the *b* or *a* axis and an offset of 0.25 along the *a* or *b* axis for the LT and RT structures, respectively. As shown in Figs. 4 and 5, the unit cell of the RT structure contains two layers of molecules centred on $z = \frac{1}{4}$ and $\frac{3}{4}$ and related to one another by the operation of crystallographic centres of symmetry, which is the only relationship between neighbouring layers as they are stacked in the *c* direction. The situation in the LT structure is more complex. As shown in Figs. 6 and 7, the unit cell of the LT structure encompasses four layers of molecules centred on $z = \frac{1}{8}, \frac{3}{8}, \frac{5}{8}$ and $\frac{7}{8}$. The layers at $z = \frac{1}{8}$ and $\frac{3}{8}$ are related to one another by the operation of crystallographic twofold screw axes, and the same is true for the layers at $z = \frac{5}{8}$ and $\frac{7}{8}$. The layers at $z = \frac{1}{8}$ and $\frac{5}{8}$ are related by the operation of crystallographic *c*-glide planes and the same is true for the layers at $z = \frac{3}{8}$ and $\frac{7}{8}$. Pairs of layers are now, of course, centred on $z = \frac{1}{4}$ and $\frac{3}{4}$ and are related to one another, as they are stacked in the *c* direction, by the operation of crystallographic centres of inversion, together with the operation of the crystallographic *c*-glide planes already mentioned.

There are no π–π interactions in the structures. Table 4 gives details of distances and angles for the most relevant close contacts between molecules. These values are indicative that

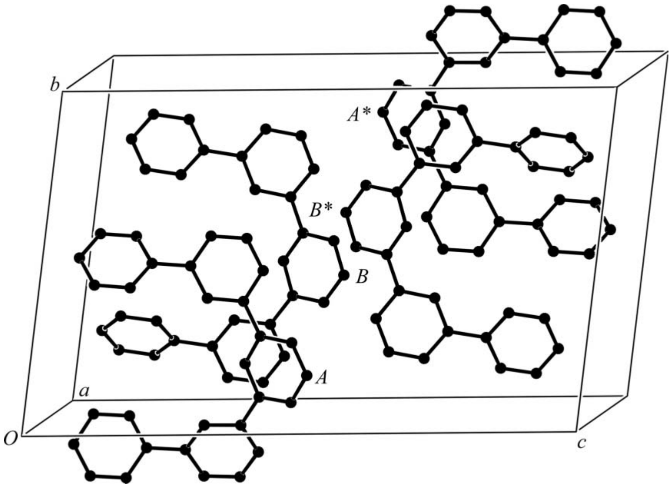

Figure 4
A view of the packing of the molecules in the unit cell of the RT form of (I), viewed along the *a* axis. H atoms have been omitted for clarity. Molecules labelled with an asterisk (*) are at the symmetry position $(-x + 1, -y + 1, -z + 1)$.

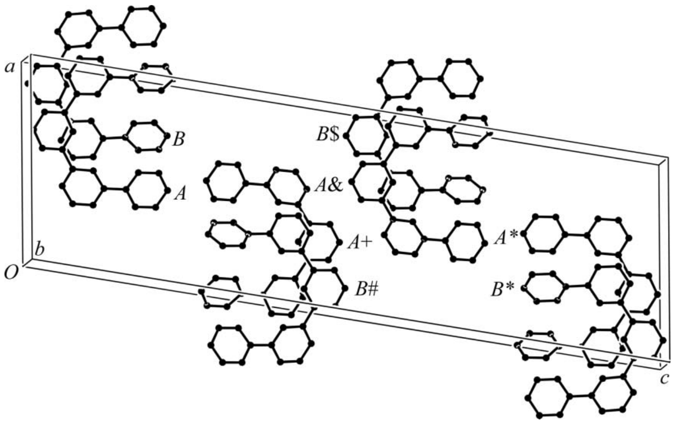

Figure 6
A view of the packing of the molecules in the unit cell of the LT form of (I), viewed along the *b* axis. H atoms have been omitted for clarity. Molecules labelled with an asterisk (*), hash (#), ampersand (&), plus sign (+) or dollar sign ($) are at the symmetry positions $(-x + 1, -y + 1, -z + 1)$, $(-x + 1, y + \frac{1}{2}, -z + \frac{1}{2})$, $(x, -y + \frac{3}{2}, z + \frac{1}{2})$, $(-x + 1, y - \frac{1}{2}, -z + \frac{1}{2})$ or $(x, -y + \frac{1}{2}, z + \frac{1}{2})$, respectively.

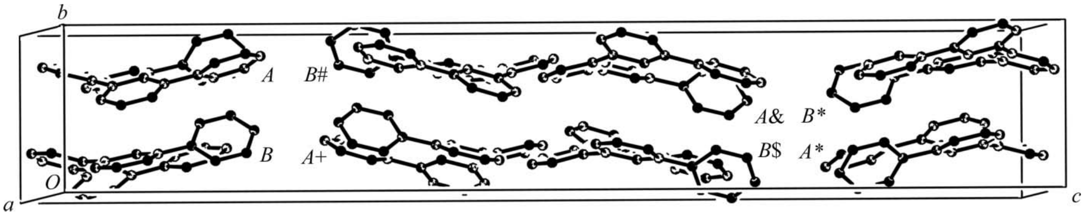

Figure 7
A view of the packing of the molecules in the unit cell of the LT form of (I), viewed along the *a* axis. H atoms have been omitted for clarity. Molecules labelled with an asterisk (*), hash (#), ampersand (&), plus sign (+) or dollar sign ($) are at the symmetry positions $(-x+1, -y+1, -z+1)$, $(-x+1, y+\frac{1}{2}, -z+\frac{1}{2})$, $(x, -y+\frac{3}{2}, z+\frac{1}{2})$, $(-x+1, y-\frac{1}{2}, -z+\frac{1}{2})$ or $(x, -y+\frac{1}{2}, z+\frac{1}{2})$, respectively.

the contacts are too weak and may not be considered as significant C—H$\cdots\pi$ interactions. Comparison of the values between polymorphs, for corresponding contacts, suggests that they are stronger in the LT polymorph. The packing motifs, molecular conformations and mutual orientations of the molecules are very similar in the two structures. Nevertheless, the LT polymorph appears to have a more efficient packing than the RT one, as suggested by the volume allocated per molecule in the LT structure (approximately 10 Å^3 less). This fact is obviously reflected in macroscopic terms by the slight differences in the values for the densities, of 1.233 (calculated) and 1.209 Mg m^{-3} (measured) (Rabideau *et al.*, 1993) in the LT and RT structures, respectively. Roughly speaking, for organic compounds, the linear thermal expansion coefficient is less than 0.0001 K^{-1}, which would give a density of about 1.19 Mg m^{-3} for the LT polymorph at room temperature, considering the temperature difference of 140 K between the measurements. The differences found in the densities may be attributed mainly to the thermal expansion of the compound, drawing attention to the role that entropy may play in the formation of the polymorphs.

This kind of polymorphism contrasts with that shown by the homologous *p*-quinquephenyl. The phase transitions in *p*-polyphenyls are well established for the case of *p*-terphenyl and *p*-quaterphenyl. Those transitions are accompanied by a change in the crystal structure (space group $P\overline{1}$ before the transition and space group $P2_1/n$ after the phase transition) associated with an energy change (heat of transition), and therefore a change in the absolute heat capacity of the compound, at the temperature of transition. The structure of the parent *p*-quinquephenyl has not been determined at low temperatures, but Saito *et al.* (2000) have suggested, based on the measurement of heat capacity excess with temperature, that the parent *p*-quinquephenyl would have a twist phase transition at about 264 K, similar to what is observed in the *p*-polyphenyls (n = 3, 4). In the case of *p*-quaterphenyl, on the basis of the available structural data [*p*-quaterphenyl at 283–303 K (R = 0.045; Delugeard *et al.*, 1976) and *p*-quaterphenyl at 110 K (R = 0.104; Baudour *et al.*, 1978)], it appears that the individual molecules have significantly different conformations in the high-temperature phase (virtually planar and centrosymmetric) and low-temperature phase (nonplanar and noncentrosymmetric). Furthermore, they each have entirely different supramolecular structures. In the case of the HT form, there are four potential but very weak C—H$\cdots\pi$ interactions (H$\cdots$*Cg* distances in the range 2.83–2.97 Å, with angles at H of 130–137°) stabilizing the supramolecular structure. In the case of the LT form, there are ten potential C—H$\cdots\pi$ interactions (H$\cdots$*Cg* distances of 2.69–2.97 Å and angles at H of 126–144°, of which eight have angles at H greater than 139°) which stabilize the packing. This is the converse of the situation for the HT and LT forms of *m*-quinquephenyl presented here, where the impact of C—H$\cdots\pi$ interactions on the supramolecular structures is minimal compared with the *p*-isomer. Also, apart from the change in torsion angles for the outer phenyl rings in molecule LT*B*, the molecular geometry is virtually unaffected. These differences may help to understand the effect of isomerization on some of the physical properties of the polyphenyls, such as melting points, or enthalpies of formation or vaporization.

Due to the simplicity of the elemental composition of polyphenyls, the only possible stabilization mechanism of their supramolecular structures is through the contribution of weak C—H$\cdots\pi$ and/or π–π interactions, thus making them good models for the study of the impact of these interactions on molecular geometry, packing or molecular motion constraints, parameters that will be reflected in their physical properties. As far as the *p*-polyphenyls are concerned, the phase change from low to high temperature leads to a reduction in the interactions and the molecular motion becomes less constrained. This may explain the high heat capacity of these compounds, which makes them good candidates for use as coolants. The molecular motion, symmetry and higher number of C—H$\cdots\pi$ interactions which the *p*-oligomers establish in relation to the *m*-oligomers may explain the higher melting points of the former. Despite that, our comparative analysis of two *m*-quinquephenyl polymorphs has highlighted the role of weak close contacts on cell volume and densities.

Experimental

m-Quinquephenyl was synthesized using the Suzuki–Miyaura aryl cross-coupling method by adapting the procedure described in the literature (Miyaura & Suzuki, 1995; Liu *et al.*, 2006). The compound was synthesized by the reaction of a mixture of 1,3-dibromobenzene (3 mmol), 3-boronic acid (11 mmol), Pd(OAc)$_2$ (0.1 mmol) and K$_2$CO$_3$ (15 mmol) in distilled water (15 ml), toluene (30 ml) and ethanol (10 ml). The mixture was stirred under a nitrogen atmosphere for approximately 10 h at 350 K. The product was purified by recrystallization from methanol and by sublimation under reduced pressure (<10 Pa). The purity of the compound was checked by gas

Table 1
Dihedral angles (°) between adjacent planes.

The angles are measured from the ring containing atom C11 (ring 1) through to that containing C51 (ring 5) in all molecules.

Rings	LT*A*	LT*B*	RT*A*	RT*B*
1–2	36.28 (11)	35.30 (12)	36.25 (9)	36.11 (9)
2–3	32.11 (11)	33.91 (11)	32.22 (8)	34.39 (8)
3–4	31.54 (11)	30.89 (12)	30.67 (8)	30.51 (9)
4–5	34.16 (12)	37.07 (13)	35.68 (10)	35.68 (10)

Table 3
Coordinates of the centroids of the molecules in the asymmetric units of the LT and RT forms of (I).

Molecule	x	y	z	Δx	Δy	Δz
LT*A*	0.6876	0.7492	0.1196			
LT*B*	0.9459	0.2502	0.1187	0.2583	0.4990	0.0009
RT*A*	0.3231	0.1872	0.2602			
RT*B*	0.8220	0.4447	0.2655	0.4989	0.2575	0.0053

chromatography, using an HP 4890 apparatus equipped with an HP-5 column [crosslinked, 5% diphenyl and 95% dimethylpolysiloxane, showing a % (*m*/*m*) purity greater than 99.8%]. The relative atomic masses used were those recommended by the IUPAC Commission in 2007 (Wieser & Berglund, 2009). Crystals suitable for X-ray diffraction were obtained by recrystallization by evaporation from a solution in methanol–acetone (3:1 *v*/*v*).

Crystal data

$C_{30}H_{22}$
$M_r = 382.48$
Monoclinic, $P2_1/c$
$a = 13.5740\ (7)$ Å
$b = 7.1809\ (4)$ Å
$c = 42.833\ (2)$ Å
$\beta = 99.274\ (4)$°
$V = 4120.5\ (4)$ Å^3
$Z = 8$
Mo $K\alpha$ radiation
$\mu = 0.07$ mm^{-1}
$T = 150$ K
$0.30 \times 0.08 \times 0.02$ mm

Data collection

Bruker APEXII CCD area-detector diffractometer
Absorption correction: multi-scan (*SADABS*; Bruker, 2004)
$T_{\min} = 0.979$, $T_{\max} = 0.999$
28626 measured reflections
8455 independent reflections
6424 reflections with $I > 2\sigma(I)$
$R_{\rm int} = 0.042$

Refinement

$R[F^2 > 2\sigma(F^2)] = 0.049$
$wR(F^2) = 0.155$
$S = 1.02$
8453 reflections
543 parameters
H-atom parameters constrained
$\Delta\rho_{\max} = 0.22$ e Å^{-3}
$\Delta\rho_{\min} = -0.27$ e Å^{-3}

H atoms were treated as riding, with aromatic C—H = 0.95 Å and $U_{\rm iso}({\rm H}) = 1.2U_{\rm eq}({\rm C})$. The positions of the H atoms were calculated and checked on a difference map during the refinement.

The crystal was a three-component nonmerohedral twin and was refined using an HKLF 5 reflection file (Sheldrick, 2008) with BASF values of 0.246 (2) and 0.0491 (3). This was discovered after an initial attempt at refinement gave a high *R* factor and the TwinRotMat option in *PLATON* (Spek, 2009) revealed the existence of three twin domains. The TwinRotMat option was used to generate the HKLF 5 reflection file from the original data, which had been integrated initially as a nontwinned data set.

The $\overline{2}0\overline{2}$, $20\overline{2}$, 200, $\overline{2}00$, $\overline{2}04$ and 102 reflections were omitted as they were obscured by the beam stop.

Data collection: *APEX2* (Bruker, 2004); cell refinement: *APEX2* and *SAINT* (Bruker, 2004); data reduction: *SAINT*; program(s) used to solve structure: *SHELXS97* (Sheldrick, 2008); program(s) used to refine structure: *SHELXL97* (Sheldrick, 2008) and *OSCAIL* (McArdle *et al.*, 2004); molecular graphics: *PLATON* (Spek, 2009); software used to prepare material for publication: *SHELXL97*.

The authors are grateful to the Fundação para a Ciência e Tecnologia (FCT), Lisbon, Portugal, and to FEDER for financial support to the Centro de Investigação em Química, University of Porto. ASMCR acknowledges financial support from FCT and the European Social Fund (ESF) under the Community Support Framework (CSF) for the award of PhD Research Grant No. SFRH/BD/81261/2011.

Supplementary data for this paper are available from the IUCr electronic archives (Reference: LN3153). Services for accessing these data are described at the back of the journal.

References

Baker, K. N., Fratini, A. V. & Adams, W. W. (1990). *Polymer*, **31**, 1623–1631.
Baudour, J.-L., Délugeard, Y. & Rivet, P. (1978). *Acta Cryst.* B**34**, 625–628.
Bruker (2004). *APEX*, *SAINT* and *SADABS*. Bruker AXS Inc., Madison, Wisconsin, USA.
Delugeard, Y., Desuche, J. & Baudour, J. L. (1976). *Acta Cryst.* B**32**, 702–705.
Kálmán, A., Párkányi, L. & Argay, G. (1993). *Acta Cryst.* B**49**, 1039–1049.
Lima, C. F. R. A. C., Rodriguez-Borges, J. E. & Santos, L. M. N. B. F. (2011). *Tetrahedron*, **67**, 689–697.
Liu, L. Y., Zhang, Y. & Xin, B. (2006). *J. Org. Chem.* **71**, 3994–3997.
Mackay, A. L. (1984). *Acta Cryst.* A**40**, 165–166.
McArdle, P., Gilligan, K., Cunningham, D., Dark, R. & Mahon, M. (2004). *CrystEngComm*, **6**, 303–309.
Miyaura, N. (2002). *Top. Curr. Chem.* **219**, 11–59.
Miyaura, A. & Suzuki, A. (1995). *Chem. Rev.* **95**, 2457–2483.

Table 2
MOLFIT parameters for overlays of all combinations of molecules from both polymorphs.

An asterisk (*) denotes an inverted molecule.

Molecule	Molecule	R.m.s. fit (weighted) (Å)	Isometricity index (weighted)	R.m.s. fit (unit weights) (Å)	Isometricity index (unit)	R.m.s. fit of bond lengths (Å)	R.m.s. fit of angles (°)	Fit rotation angle (°)
LT*A**	LT*B*	0.044	95.6	0.038	96.2	0.0045	0.297	179.68
RT*A**	RT*B*	0.053	94.7	0.049	95.1	0.0042	0.270	179.79
LT*A**	RT*A*	0.036	96.4	0.032	96.8	0.0065	0.353	89.91
LT*A*	RT*B*	0.063	93.7	0.060	94.0	0.0066	0.332	179.69
LT*B*	RT*A*	0.037	96.3	0.036	96.4	0.0072	0.316	−179.72
LT*B**	RT*B*	0.061	93.9	0.054	94.6	0.0076	0.292	−90.58

Table 4
Short contacts (Å, °) between molecules.

Cg is the centre of gravity of the ring containing the indicated atom.

Polymorph	C	H	Ring (pivot atom)	Symmetry operator for ring	C—H	H$\cdots$*Cg*	C$\cdots$*Cg*	Angle at H
LT	C53*B*	H53*B*	*Cg* (C51*A*)	x, y, z	0.95	2.96	3.801 (3)	149
LT	C25*B*	H25*B*	*Cg* (C21*A*)	$x + 1, y - 1, z$	0.95	2.91	3.521 (3)	123
LT	C15*A*	H15*A*	*Cg* (C11*B*)	$x - 1, y + 1, z$	0.95	3.00	3.451 (3)	111
LT	C46*A*	H46*A*	*Cg* (C31*B*)	x, y, z	0.95	2.95	3.354 (2)	107
LT	C46*B*	H46*B*	*Cg* (C31*A*)	$x, y - 1, z$	0.95	3.00	3.319 (3)	101
RT	C53*B*	H53*B*	*Cg* (C51*A*)	$x, y - 1, z$	0.97	3.03	3.867	145
RT	C25*B*	H25*B*	*Cg* (C21*A*)	$x + 1, y + 1, z$	1.03	2.97	3.606	122
RT	C15*A*	H15*A*	*Cg* (C11*B*)	$x - 1, y - 1, z$	0.95	3.12	3.503	107
RT	C46*A*	H46*A*	*Cg* (C31*B*)	x, y, z	1.00	2.97	3.404	107
RT	C46*B*	H46*B*	*Cg* (C31*A*)	$x + 1, y, z$	0.99	3.06	3.346	98

Rabideau, P. W., Sygula, A., Dhar, R. K. & Fronczek, F. (1993). *Chem. Commun.* pp. 1795–1797.

Saito, K., Yamamura, Y. & Sorai, M. (2000). *Bull. Chem. Soc. Jpn*, **73**, 2713–2718.

Sheldrick, G. M. (2008). *Acta Cryst.* A**64**, 112–122.

Spek, A. L. (2009). *Acta Cryst.* D**65**, 148–155.

Suzuki, A. (2011). *Angew. Chem. Int. Ed.* **50**, 6722–6737.

Wieser, M. E. & Berglund, M. (2009). *Pure Appl. Chem.* **81**, 2131–2156.

supplementary materials

Acta Cryst. (2012). C**68**, o492–o497 [doi:10.1107/S0108270112046392]

A low-temperature polymorph of *m*-quinquephenyl

Ligia R. Gomes, R. Alan Howie, John Nicolson Low, Ana S. M. C. Rodrigues and Luís M. N. B. F. Santos

1,1′:3′,1″:3″,1‴:3‴,1⁗-quinquephenyl

Crystal data

$C_{30}H_{22}$
$M_r = 382.48$
Monoclinic, $P2_1/c$
Hall symbol: -P 2ybc
$a = 13.5740$ (7) Å
$b = 7.1809$ (4) Å
$c = 42.833$ (2) Å
$\beta = 99.274$ (4)°
$V = 4120.5$ (4) Å^3
$Z = 8$

$F(000) = 1616$
$D_x = 1.233$ Mg m^{-3}
Mo $K\alpha$ radiation, $\lambda = 0.71073$ Å
Cell parameters from 28626 reflections
$\theta = 2.9$–26.5°
$\mu = 0.07$ mm^{-1}
$T = 150$ K
Needle, colourless
0.30 × 0.08 × 0.02 mm

Data collection

Bruker APEXII CCD area-detector diffractometer
Radiation source: fine-focus sealed tube
Graphite monochromator
Detector resolution: 8.33 pixels mm^{-1}
ω scans
Absorption correction: multi-scan (*SADABS*; Bruker, 2004)
$T_{min} = 0.979$, $T_{max} = 0.999$

28626 measured reflections
8455 independent reflections
6424 reflections with $I > 2\sigma(I)$
$R_{int} = 0.042$
$\theta_{max} = 26.5°$, $\theta_{min} = 2.9°$
$h = -17 \rightarrow 16$
$k = -9 \rightarrow 9$
$l = -53 \rightarrow 15$

Refinement

Refinement on F^2
Least-squares matrix: full
$R[F^2 > 2\sigma(F^2)] = 0.049$
$wR(F^2) = 0.155$
$S = 1.02$
8453 reflections
543 parameters
0 restraints
Primary atom site location: structure-invariant direct methods

Secondary atom site location: difference Fourier map
Hydrogen site location: inferred from neighbouring sites
H-atom parameters constrained
$w = 1/[\sigma^2(F_o^2) + (0.0988P)^2]$ where $P = (F_o^2 + 2F_c^2)/3$
$(\Delta/\sigma)_{max} = 0.001$
$\Delta\rho_{max} = 0.22$ e Å^{-3}
$\Delta\rho_{min} = -0.27$ e Å^{-3}

Special details

Geometry. All e.s.d.'s (except the e.s.d. in the dihedral angle between two l.s. planes) are estimated using the full covariance matrix. The cell e.s.d.'s are taken into account individually in the estimation of e.s.d.'s in distances, angles and torsion angles; correlations between e.s.d.'s in cell parameters are only used when they are defined by crystal symmetry. An approximate (isotropic) treatment of cell e.s.d.'s is used for estimating e.s.d.'s involving l.s. planes.

Refinement. Refinement of F^2 against ALL reflections. The weighted R-factor wR and goodness of fit S are based on F^2, conventional R-factors R are based on F, with F set to zero for negative F^2. The threshold expression of $F^2 > \sigma(F^2)$ is used only for calculating R-factors(gt) *etc*. and is not relevant to the choice of reflections for refinement. R-factors based on F^2 are statistically about twice as large as those based on F, and R-factors based on ALL data will be even larger.

Fractional atomic coordinates and isotropic or equivalent isotropic displacement parameters (Å²)

	x	y	z	U_{iso}*/U_{eq}
C11A	0.42665 (17)	0.7263 (3)	0.15232 (5)	0.0275 (5)
C12A	0.51917 (18)	0.7150 (4)	0.17196 (5)	0.0339 (6)
H12A	0.5753	0.6695	0.1636	0.041*
C13A	0.5304 (2)	0.7688 (4)	0.20333 (6)	0.0409 (6)
H13A	0.5937	0.7587	0.2164	0.049*
C14A	0.4496 (2)	0.8374 (4)	0.21572 (6)	0.0419 (7)
H14A	0.4576	0.8785	0.2371	0.050*
C15A	0.3572 (2)	0.8456 (4)	0.19677 (5)	0.0396 (6)
H15A	0.3011	0.8894	0.2053	0.048*
C16A	0.34562 (18)	0.7908 (3)	0.16549 (5)	0.0324 (5)
H16A	0.2815	0.7970	0.1528	0.039*
C21A	0.41579 (16)	0.6744 (3)	0.11825 (5)	0.0253 (5)
C22A	0.49255 (16)	0.7142 (3)	0.10122 (5)	0.0261 (5)
H22A	0.5506	0.7761	0.1116	0.031*
C23A	0.48663 (16)	0.6657 (3)	0.06951 (5)	0.0259 (5)
C24A	0.39996 (17)	0.5785 (3)	0.05429 (5)	0.0306 (5)
H24A	0.3941	0.5452	0.0326	0.037*
C25A	0.32251 (17)	0.5406 (3)	0.07084 (5)	0.0325 (5)
H25A	0.2636	0.4818	0.0604	0.039*
C26A	0.33005 (17)	0.5873 (3)	0.10237 (5)	0.0291 (5)
H26A	0.2764	0.5600	0.1134	0.035*
C31A	0.57269 (17)	0.7040 (3)	0.05304 (5)	0.0271 (5)
C32A	0.66903 (16)	0.6970 (3)	0.06998 (5)	0.0243 (5)
H32A	0.6777	0.6626	0.0917	0.029*
C33A	0.75358 (17)	0.7381 (3)	0.05658 (5)	0.0261 (5)
C34A	0.73898 (19)	0.7850 (3)	0.02437 (5)	0.0309 (5)
H34A	0.7948	0.8152	0.0145	0.037*
C35A	0.6439 (2)	0.7877 (4)	0.00687 (5)	0.0363 (6)
H35A	0.6352	0.8170	−0.0150	0.044*
C36A	0.56147 (18)	0.7482 (4)	0.02089 (5)	0.0325 (6)
H36A	0.4967	0.7512	0.0086	0.039*
C41A	0.85465 (17)	0.7337 (3)	0.07602 (5)	0.0248 (5)
C42A	0.86803 (17)	0.7796 (3)	0.10822 (5)	0.0254 (5)
H42A	0.8116	0.8152	0.1174	0.030*
C43A	0.96152 (17)	0.7749 (3)	0.12728 (5)	0.0265 (5)
C44A	1.04363 (17)	0.7258 (3)	0.11342 (5)	0.0309 (5)
H44A	1.1082	0.7238	0.1259	0.037*

C45A	1.03228 (18)	0.6799 (4)	0.08169 (5)	0.0336 (6)
H45A	1.0890	0.6464	0.0725	0.040*
C46A	0.93914 (18)	0.6825 (3)	0.06326 (5)	0.0309 (5)
H46A	0.9323	0.6489	0.0416	0.037*
C51A	0.97332 (17)	0.8216 (3)	0.16150 (5)	0.0285 (5)
C52A	0.91403 (18)	0.9567 (4)	0.17280 (5)	0.0329 (5)
H52A	0.8646	1.0196	0.1584	0.039*
C53A	0.9262 (2)	1.0006 (4)	0.20470 (5)	0.0421 (7)
H53A	0.8852	1.0930	0.2120	0.051*
C54A	0.9979 (2)	0.9097 (4)	0.22598 (6)	0.0436 (7)
H54A	1.0062	0.9393	0.2479	0.052*
C55A	1.0573 (2)	0.7761 (4)	0.21525 (5)	0.0398 (6)
H55A	1.1070	0.7143	0.2298	0.048*
C56A	1.04489 (18)	0.7315 (4)	0.18329 (5)	0.0337 (6)
H56A	1.0858	0.6382	0.1762	0.040*
C11B	1.23715 (18)	0.2329 (3)	0.15439 (5)	0.0304 (5)
C12B	1.16226 (19)	0.2218 (3)	0.17298 (5)	0.0337 (6)
H12B	1.0981	0.1773	0.1639	0.040*
C13B	1.1797 (2)	0.2747 (4)	0.20446 (5)	0.0418 (7)
H13B	1.1277	0.2659	0.2168	0.050*
C14B	1.2732 (2)	0.3407 (4)	0.21809 (6)	0.0465 (7)
H14B	1.2849	0.3792	0.2396	0.056*
C15B	1.3488 (2)	0.3497 (4)	0.20014 (6)	0.0464 (7)
H15B	1.4130	0.3928	0.2094	0.056*
C16B	1.33127 (19)	0.2963 (4)	0.16878 (6)	0.0385 (6)
H16B	1.3841	0.3027	0.1567	0.046*
C21B	1.21749 (17)	0.1790 (3)	0.12044 (5)	0.0278 (5)
C22B	1.12411 (17)	0.2146 (3)	0.10239 (5)	0.0272 (5)
H22B	1.0748	0.2758	0.1121	0.033*
C23B	1.10068 (17)	0.1635 (3)	0.07061 (5)	0.0276 (5)
C24B	1.17384 (19)	0.0753 (3)	0.05660 (5)	0.0335 (6)
H24B	1.1597	0.0389	0.0350	0.040*
C25B	1.26747 (19)	0.0403 (4)	0.07411 (6)	0.0351 (6)
H25B	1.3169	−0.0201	0.0643	0.042*
C26B	1.28958 (18)	0.0923 (3)	0.10552 (5)	0.0329 (5)
H26B	1.3542	0.0689	0.1171	0.039*
C31B	0.99907 (18)	0.2009 (3)	0.05315 (5)	0.0286 (5)
C32B	0.91739 (17)	0.1939 (3)	0.06889 (5)	0.0259 (5)
H32B	0.9279	0.1582	0.0905	0.031*
C33B	0.82084 (18)	0.2366 (3)	0.05441 (5)	0.0285 (5)
C34B	0.8064 (2)	0.2864 (3)	0.02240 (5)	0.0356 (6)
H34B	0.7415	0.3178	0.0118	0.043*
C35B	0.8863 (2)	0.2897 (4)	0.00617 (5)	0.0404 (7)
H35B	0.8754	0.3206	−0.0157	0.048*
C36B	0.9814 (2)	0.2493 (4)	0.02097 (5)	0.0365 (6)
H36B	1.0354	0.2542	0.0094	0.044*
C41B	0.73715 (17)	0.2329 (3)	0.07294 (5)	0.0283 (5)
C42B	0.75414 (17)	0.2748 (3)	0.10511 (5)	0.0273 (5)
H42B	0.8198	0.3068	0.1149	0.033*

C43B	0.67802 (17)	0.2713 (3)	0.12340 (5)	0.0300 (5)
C44B	0.58204 (19)	0.2254 (4)	0.10854 (6)	0.0375 (6)
H44B	0.5288	0.2225	0.1205	0.045*
C45B	0.56377 (19)	0.1843 (4)	0.07672 (6)	0.0396 (6)
H45B	0.4979	0.1538	0.0669	0.048*
C46B	0.63964 (18)	0.1867 (4)	0.05895 (5)	0.0342 (6)
H46B	0.6259	0.1569	0.0371	0.041*
C51B	0.69879 (17)	0.3198 (4)	0.15763 (5)	0.0311 (5)
C52B	0.76721 (18)	0.4578 (4)	0.16903 (5)	0.0331 (6)
H52B	0.8021	0.5211	0.1547	0.040*
C53B	0.7855 (2)	0.5049 (4)	0.20080 (5)	0.0415 (6)
H53B	0.8321	0.6003	0.2080	0.050*
C54B	0.7358 (2)	0.4127 (4)	0.22196 (6)	0.0470 (7)
H54B	0.7477	0.4449	0.2438	0.056*
C55B	0.6686 (2)	0.2728 (4)	0.21110 (6)	0.0477 (7)
H55B	0.6347	0.2085	0.2256	0.057*
C56B	0.6506 (2)	0.2261 (4)	0.17936 (6)	0.0405 (6)
H56B	0.6048	0.1291	0.1723	0.049*

Atomic displacement parameters (Å²)

	U^{11}	U^{22}	U^{33}	U^{12}	U^{13}	U^{23}
C11A	0.0309 (12)	0.0237 (13)	0.0284 (11)	−0.0015 (10)	0.0065 (9)	0.0036 (9)
C12A	0.0314 (13)	0.0375 (15)	0.0325 (12)	−0.0010 (11)	0.0042 (10)	0.0000 (11)
C13A	0.0428 (15)	0.0443 (17)	0.0331 (13)	−0.0040 (13)	−0.0011 (11)	−0.0004 (11)
C14A	0.0567 (17)	0.0425 (17)	0.0272 (12)	−0.0016 (14)	0.0094 (12)	−0.0011 (11)
C15A	0.0484 (15)	0.0392 (16)	0.0348 (13)	0.0080 (13)	0.0177 (11)	0.0064 (11)
C16A	0.0335 (13)	0.0297 (14)	0.0342 (12)	0.0018 (11)	0.0064 (10)	0.0067 (10)
C21A	0.0249 (11)	0.0191 (12)	0.0305 (11)	0.0018 (9)	0.0004 (9)	0.0034 (9)
C22A	0.0239 (11)	0.0240 (13)	0.0290 (11)	0.0006 (10)	−0.0002 (9)	−0.0001 (9)
C23A	0.0277 (12)	0.0209 (12)	0.0270 (11)	0.0035 (10)	−0.0014 (9)	0.0013 (9)
C24A	0.0336 (13)	0.0265 (13)	0.0286 (11)	0.0009 (10)	−0.0041 (9)	−0.0014 (10)
C25A	0.0268 (12)	0.0269 (13)	0.0405 (13)	−0.0013 (10)	−0.0048 (10)	0.0000 (10)
C26A	0.0262 (11)	0.0248 (13)	0.0353 (12)	0.0006 (10)	0.0021 (9)	0.0050 (10)
C31A	0.0345 (12)	0.0223 (12)	0.0233 (10)	0.0005 (10)	0.0014 (9)	−0.0034 (9)
C32A	0.0340 (12)	0.0220 (12)	0.0168 (9)	0.0017 (10)	0.0037 (8)	0.0003 (8)
C33A	0.0373 (13)	0.0199 (12)	0.0221 (10)	0.0022 (10)	0.0080 (9)	0.0005 (8)
C34A	0.0445 (14)	0.0295 (14)	0.0206 (10)	0.0008 (11)	0.0107 (10)	−0.0007 (9)
C35A	0.0534 (15)	0.0365 (16)	0.0185 (11)	0.0011 (13)	0.0043 (10)	0.0009 (10)
C36A	0.0382 (13)	0.0340 (14)	0.0222 (11)	0.0008 (11)	−0.0046 (9)	0.0005 (9)
C41A	0.0329 (12)	0.0191 (12)	0.0240 (10)	0.0005 (10)	0.0094 (9)	0.0032 (8)
C42A	0.0302 (11)	0.0224 (12)	0.0249 (10)	0.0006 (10)	0.0088 (9)	0.0031 (9)
C43A	0.0310 (12)	0.0218 (12)	0.0269 (11)	−0.0013 (10)	0.0052 (9)	0.0032 (9)
C44A	0.0254 (11)	0.0325 (14)	0.0346 (12)	−0.0008 (11)	0.0041 (9)	0.0019 (10)
C45A	0.0322 (13)	0.0345 (14)	0.0376 (13)	0.0029 (11)	0.0161 (10)	0.0011 (11)
C46A	0.0405 (14)	0.0277 (13)	0.0278 (11)	−0.0008 (11)	0.0154 (10)	−0.0001 (10)
C51A	0.0268 (11)	0.0282 (13)	0.0300 (11)	−0.0040 (10)	0.0035 (9)	0.0015 (10)
C52A	0.0326 (13)	0.0360 (15)	0.0291 (12)	0.0054 (11)	0.0020 (9)	−0.0015 (10)
C53A	0.0434 (15)	0.0498 (18)	0.0330 (13)	0.0016 (13)	0.0055 (11)	−0.0103 (12)
C54A	0.0519 (16)	0.0514 (18)	0.0258 (12)	−0.0068 (14)	0.0010 (11)	−0.0051 (11)

C55A	0.0390 (14)	0.0443 (17)	0.0323 (12)	−0.0024 (13)	−0.0056 (11)	0.0062 (11)
C56A	0.0333 (13)	0.0313 (14)	0.0354 (12)	−0.0008 (11)	0.0022 (10)	0.0021 (10)
C11B	0.0323 (12)	0.0234 (13)	0.0348 (12)	−0.0012 (10)	0.0030 (10)	0.0081 (10)
C12B	0.0356 (13)	0.0303 (14)	0.0343 (12)	0.0030 (11)	0.0033 (10)	0.0018 (10)
C13B	0.0531 (16)	0.0390 (17)	0.0328 (13)	0.0066 (13)	0.0049 (12)	0.0049 (11)
C14B	0.069 (2)	0.0340 (16)	0.0307 (13)	0.0040 (14)	−0.0096 (13)	0.0015 (11)
C15B	0.0513 (17)	0.0342 (16)	0.0470 (15)	−0.0056 (14)	−0.0120 (12)	0.0093 (12)
C16B	0.0375 (14)	0.0322 (15)	0.0433 (14)	−0.0026 (12)	−0.0014 (11)	0.0108 (11)
C21B	0.0308 (12)	0.0206 (12)	0.0336 (12)	−0.0035 (10)	0.0097 (9)	0.0065 (9)
C22B	0.0323 (12)	0.0224 (13)	0.0288 (11)	−0.0011 (10)	0.0106 (9)	0.0020 (9)
C23B	0.0353 (13)	0.0213 (12)	0.0283 (11)	−0.0022 (10)	0.0112 (9)	0.0011 (9)
C24B	0.0460 (14)	0.0239 (13)	0.0343 (12)	−0.0038 (11)	0.0176 (11)	0.0008 (10)
C25B	0.0393 (14)	0.0256 (14)	0.0454 (14)	0.0043 (11)	0.0215 (11)	0.0066 (11)
C26B	0.0302 (12)	0.0256 (14)	0.0449 (14)	0.0016 (11)	0.0121 (10)	0.0072 (10)
C31B	0.0416 (13)	0.0201 (12)	0.0249 (11)	−0.0017 (10)	0.0083 (9)	−0.0007 (9)
C32B	0.0359 (12)	0.0207 (12)	0.0197 (10)	−0.0023 (10)	0.0003 (9)	0.0018 (8)
C33B	0.0368 (13)	0.0199 (12)	0.0269 (11)	−0.0018 (10)	−0.0004 (9)	−0.0022 (9)
C34B	0.0478 (15)	0.0308 (15)	0.0246 (11)	−0.0001 (12)	−0.0050 (10)	−0.0012 (10)
C35B	0.0599 (17)	0.0397 (17)	0.0201 (11)	−0.0001 (13)	0.0023 (11)	−0.0003 (10)
C36B	0.0523 (16)	0.0337 (15)	0.0251 (11)	−0.0008 (12)	0.0113 (11)	−0.0014 (10)
C41B	0.0321 (12)	0.0186 (12)	0.0312 (11)	0.0019 (10)	−0.0042 (9)	0.0035 (9)
C42B	0.0267 (11)	0.0226 (13)	0.0313 (11)	0.0012 (10)	0.0006 (9)	0.0024 (9)
C43B	0.0293 (12)	0.0219 (13)	0.0380 (12)	0.0010 (10)	0.0031 (10)	0.0033 (10)
C44B	0.0276 (12)	0.0273 (14)	0.0579 (16)	0.0022 (11)	0.0074 (11)	0.0018 (11)
C45B	0.0261 (13)	0.0309 (15)	0.0566 (16)	−0.0004 (11)	−0.0094 (11)	−0.0031 (12)
C46B	0.0330 (13)	0.0285 (14)	0.0370 (13)	0.0028 (11)	−0.0069 (10)	−0.0018 (10)
C51B	0.0282 (12)	0.0288 (14)	0.0381 (12)	0.0048 (11)	0.0109 (10)	0.0047 (10)
C52B	0.0326 (13)	0.0359 (15)	0.0318 (12)	0.0023 (11)	0.0087 (10)	0.0035 (10)
C53B	0.0414 (15)	0.0477 (17)	0.0358 (13)	0.0022 (13)	0.0074 (11)	−0.0030 (11)
C54B	0.0562 (17)	0.0526 (19)	0.0347 (13)	0.0138 (15)	0.0149 (12)	0.0055 (13)
C55B	0.0569 (18)	0.0451 (18)	0.0478 (15)	0.0113 (15)	0.0284 (14)	0.0117 (13)
C56B	0.0411 (15)	0.0351 (16)	0.0501 (15)	0.0030 (12)	0.0216 (12)	0.0061 (12)

Geometric parameters (Å, º)

C11A—C16A	1.394 (3)	C11B—C12B	1.391 (3)
C11A—C12A	1.397 (3)	C11B—C16B	1.402 (3)
C11A—C21A	1.490 (3)	C11B—C21B	1.487 (3)
C12A—C13A	1.383 (3)	C12B—C13B	1.384 (3)
C12A—H12A	0.9500	C12B—H12B	0.9500
C13A—C14A	1.384 (4)	C13B—C14B	1.393 (4)
C13A—H13A	0.9500	C13B—H13B	0.9500
C14A—C15A	1.381 (4)	C14B—C15B	1.379 (4)
C14A—H14A	0.9500	C14B—H14B	0.9500
C15A—C16A	1.381 (3)	C15B—C16B	1.380 (4)
C15A—H15A	0.9500	C15B—H15B	0.9500
C16A—H16A	0.9500	C16B—H16B	0.9500
C21A—C22A	1.394 (3)	C21B—C22B	1.398 (3)
C21A—C26A	1.398 (3)	C21B—C26B	1.398 (3)
C22A—C23A	1.392 (3)	C22B—C23B	1.396 (3)

C22A—H22A	0.9500	C22B—H22B	0.9500
C23A—C24A	1.398 (3)	C23B—C24B	1.393 (3)
C23A—C31A	1.484 (3)	C23B—C31B	1.484 (3)
C24A—C25A	1.386 (3)	C24B—C25B	1.390 (3)
C24A—H24A	0.9500	C24B—H24B	0.9500
C25A—C26A	1.379 (3)	C25B—C26B	1.382 (3)
C25A—H25A	0.9500	C25B—H25B	0.9500
C26A—H26A	0.9500	C26B—H26B	0.9500
C31A—C32A	1.391 (3)	C31B—C32B	1.388 (3)
C31A—C36A	1.397 (3)	C31B—C36B	1.404 (3)
C32A—C33A	1.395 (3)	C32B—C33B	1.391 (3)
C32A—H32A	0.9500	C32B—H32B	0.9500
C33A—C34A	1.403 (3)	C33B—C34B	1.400 (3)
C33A—C41A	1.486 (3)	C33B—C41B	1.487 (3)
C34A—C35A	1.384 (3)	C34B—C35B	1.380 (4)
C34A—H34A	0.9500	C34B—H34B	0.9500
C35A—C36A	1.382 (3)	C35B—C36B	1.374 (4)
C35A—H35A	0.9500	C35B—H35B	0.9500
C36A—H36A	0.9500	C36B—H36B	0.9500
C41A—C46A	1.397 (3)	C41B—C42B	1.393 (3)
C41A—C42A	1.401 (3)	C41B—C46B	1.402 (3)
C42A—C43A	1.395 (3)	C42B—C43B	1.394 (3)
C42A—H42A	0.9500	C42B—H42B	0.9500
C43A—C44A	1.390 (3)	C43B—C44B	1.394 (3)
C43A—C51A	1.487 (3)	C43B—C51B	1.489 (3)
C44A—C45A	1.383 (3)	C44B—C45B	1.377 (3)
C44A—H44A	0.9500	C44B—H44B	0.9500
C45A—C46A	1.379 (3)	C45B—C46B	1.376 (4)
C45A—H45A	0.9500	C45B—H45B	0.9500
C46A—H46A	0.9500	C46B—H46B	0.9500
C51A—C56A	1.393 (3)	C51B—C52B	1.392 (3)
C51A—C52A	1.396 (3)	C51B—C56B	1.394 (3)
C52A—C53A	1.386 (3)	C52B—C53B	1.385 (3)
C52A—H52A	0.9500	C52B—H52B	0.9500
C53A—C54A	1.385 (4)	C53B—C54B	1.383 (4)
C53A—H53A	0.9500	C53B—H53B	0.9500
C54A—C55A	1.379 (4)	C54B—C55B	1.386 (4)
C54A—H54A	0.9500	C54B—H54B	0.9500
C55A—C56A	1.389 (3)	C55B—C56B	1.383 (4)
C55A—H55A	0.9500	C55B—H55B	0.9500
C56A—H56A	0.9500	C56B—H56B	0.9500

C16A—C11A—C12A	117.9 (2)	C12B—C11B—C16B	117.7 (2)
C16A—C11A—C21A	121.3 (2)	C12B—C11B—C21B	120.8 (2)
C12A—C11A—C21A	120.8 (2)	C16B—C11B—C21B	121.4 (2)
C13A—C12A—C11A	121.1 (2)	C13B—C12B—C11B	121.1 (2)
C13A—C12A—H12A	119.5	C13B—C12B—H12B	119.5
C11A—C12A—H12A	119.5	C11B—C12B—H12B	119.5
C12A—C13A—C14A	120.1 (2)	C12B—C13B—C14B	120.2 (3)

C12A—C13A—H13A	119.9	C12B—C13B—H13B	119.9
C14A—C13A—H13A	119.9	C14B—C13B—H13B	119.9
C15A—C14A—C13A	119.4 (2)	C15B—C14B—C13B	119.5 (2)
C15A—C14A—H14A	120.3	C15B—C14B—H14B	120.3
C13A—C14A—H14A	120.3	C13B—C14B—H14B	120.3
C16A—C15A—C14A	120.6 (2)	C14B—C15B—C16B	120.2 (3)
C16A—C15A—H15A	119.7	C14B—C15B—H15B	119.9
C14A—C15A—H15A	119.7	C16B—C15B—H15B	119.9
C15A—C16A—C11A	120.9 (2)	C15B—C16B—C11B	121.3 (2)
C15A—C16A—H16A	119.5	C15B—C16B—H16B	119.3
C11A—C16A—H16A	119.5	C11B—C16B—H16B	119.3
C22A—C21A—C26A	118.09 (19)	C22B—C21B—C26B	117.9 (2)
C22A—C21A—C11A	119.79 (19)	C22B—C21B—C11B	119.8 (2)
C26A—C21A—C11A	122.12 (19)	C26B—C21B—C11B	122.3 (2)
C23A—C22A—C21A	121.9 (2)	C23B—C22B—C21B	122.3 (2)
C23A—C22A—H22A	119.0	C23B—C22B—H22B	118.8
C21A—C22A—H22A	119.0	C21B—C22B—H22B	118.8
C22A—C23A—C24A	118.6 (2)	C24B—C23B—C22B	118.3 (2)
C22A—C23A—C31A	119.44 (19)	C24B—C23B—C31B	122.3 (2)
C24A—C23A—C31A	121.94 (19)	C22B—C23B—C31B	119.40 (19)
C25A—C24A—C23A	120.0 (2)	C25B—C24B—C23B	120.2 (2)
C25A—C24A—H24A	120.0	C25B—C24B—H24B	119.9
C23A—C24A—H24A	120.0	C23B—C24B—H24B	119.9
C26A—C25A—C24A	120.7 (2)	C26B—C25B—C24B	120.8 (2)
C26A—C25A—H25A	119.7	C26B—C25B—H25B	119.6
C24A—C25A—H25A	119.7	C24B—C25B—H25B	119.6
C25A—C26A—C21A	120.7 (2)	C25B—C26B—C21B	120.5 (2)
C25A—C26A—H26A	119.7	C25B—C26B—H26B	119.8
C21A—C26A—H26A	119.7	C21B—C26B—H26B	119.8
C32A—C31A—C36A	117.8 (2)	C32B—C31B—C36B	117.5 (2)
C32A—C31A—C23A	119.41 (17)	C32B—C31B—C23B	119.94 (18)
C36A—C31A—C23A	122.8 (2)	C36B—C31B—C23B	122.5 (2)
C31A—C32A—C33A	122.98 (18)	C31B—C32B—C33B	122.97 (19)
C31A—C32A—H32A	118.5	C31B—C32B—H32B	118.5
C33A—C32A—H32A	118.5	C33B—C32B—H32B	118.5
C32A—C33A—C34A	117.4 (2)	C32B—C33B—C34B	117.8 (2)
C32A—C33A—C41A	120.76 (17)	C32B—C33B—C41B	120.25 (18)
C34A—C33A—C41A	121.83 (19)	C34B—C33B—C41B	121.9 (2)
C35A—C34A—C33A	120.5 (2)	C35B—C34B—C33B	120.0 (2)
C35A—C34A—H34A	119.8	C35B—C34B—H34B	120.0
C33A—C34A—H34A	119.8	C33B—C34B—H34B	120.0
C36A—C35A—C34A	120.77 (19)	C36B—C35B—C34B	121.3 (2)
C36A—C35A—H35A	119.6	C36B—C35B—H35B	119.3
C34A—C35A—H35A	119.6	C34B—C35B—H35B	119.3
C35A—C36A—C31A	120.5 (2)	C35B—C36B—C31B	120.3 (2)
C35A—C36A—H36A	119.8	C35B—C36B—H36B	119.9
C31A—C36A—H36A	119.8	C31B—C36B—H36B	119.9
C46A—C41A—C42A	117.6 (2)	C42B—C41B—C46B	117.9 (2)
C46A—C41A—C33A	121.90 (18)	C42B—C41B—C33B	120.3 (2)

C42A—C41A—C33A	120.53 (18)	C46B—C41B—C33B	121.73 (19)
C43A—C42A—C41A	122.1 (2)	C41B—C42B—C43B	122.2 (2)
C43A—C42A—H42A	118.9	C41B—C42B—H42B	118.9
C41A—C42A—H42A	118.9	C43B—C42B—H42B	118.9
C44A—C43A—C42A	118.21 (19)	C42B—C43B—C44B	118.0 (2)
C44A—C43A—C51A	120.8 (2)	C42B—C43B—C51B	120.6 (2)
C42A—C43A—C51A	121.01 (19)	C44B—C43B—C51B	121.3 (2)
C45A—C44A—C43A	120.7 (2)	C45B—C44B—C43B	120.6 (2)
C45A—C44A—H44A	119.7	C45B—C44B—H44B	119.7
C43A—C44A—H44A	119.7	C43B—C44B—H44B	119.7
C46A—C45A—C44A	120.4 (2)	C46B—C45B—C44B	120.9 (2)
C46A—C45A—H45A	119.8	C46B—C45B—H45B	119.6
C44A—C45A—H45A	119.8	C44B—C45B—H45B	119.6
C45A—C46A—C41A	121.0 (2)	C45B—C46B—C41B	120.4 (2)
C45A—C46A—H46A	119.5	C45B—C46B—H46B	119.8
C41A—C46A—H46A	119.5	C41B—C46B—H46B	119.8
C56A—C51A—C52A	118.0 (2)	C52B—C51B—C56B	117.9 (2)
C56A—C51A—C43A	120.5 (2)	C52B—C51B—C43B	121.5 (2)
C52A—C51A—C43A	121.5 (2)	C56B—C51B—C43B	120.7 (2)
C53A—C52A—C51A	121.1 (2)	C53B—C52B—C51B	121.5 (2)
C53A—C52A—H52A	119.5	C53B—C52B—H52B	119.2
C51A—C52A—H52A	119.5	C51B—C52B—H52B	119.2
C54A—C53A—C52A	120.0 (2)	C54B—C53B—C52B	119.8 (3)
C54A—C53A—H53A	120.0	C54B—C53B—H53B	120.1
C52A—C53A—H53A	120.0	C52B—C53B—H53B	120.1
C55A—C54A—C53A	119.7 (2)	C53B—C54B—C55B	119.4 (2)
C55A—C54A—H54A	120.1	C53B—C54B—H54B	120.3
C53A—C54A—H54A	120.1	C55B—C54B—H54B	120.3
C54A—C55A—C56A	120.3 (2)	C56B—C55B—C54B	120.6 (2)
C54A—C55A—H55A	119.9	C56B—C55B—H55B	119.7
C56A—C55A—H55A	119.9	C54B—C55B—H55B	119.7
C55A—C56A—C51A	120.9 (2)	C55B—C56B—C51B	120.7 (3)
C55A—C56A—H56A	119.5	C55B—C56B—H56B	119.6
C51A—C56A—H56A	119.5	C51B—C56B—H56B	119.6

C16A—C11A—C12A—C13A	−1.0 (4)	C16B—C11B—C12B—C13B	1.1 (4)
C21A—C11A—C12A—C13A	177.8 (2)	C21B—C11B—C12B—C13B	−178.9 (2)
C11A—C12A—C13A—C14A	−0.8 (4)	C11B—C12B—C13B—C14B	0.2 (4)
C12A—C13A—C14A—C15A	2.2 (4)	C12B—C13B—C14B—C15B	−1.2 (4)
C13A—C14A—C15A—C16A	−1.7 (4)	C13B—C14B—C15B—C16B	1.0 (4)
C14A—C15A—C16A—C11A	−0.1 (4)	C14B—C15B—C16B—C11B	0.3 (4)
C12A—C11A—C16A—C15A	1.5 (4)	C12B—C11B—C16B—C15B	−1.3 (4)
C21A—C11A—C16A—C15A	−177.4 (2)	C21B—C11B—C16B—C15B	178.7 (2)
C16A—C11A—C21A—C22A	142.8 (2)	C12B—C11B—C21B—C22B	35.2 (3)
C12A—C11A—C21A—C22A	−36.0 (3)	C16B—C11B—C21B—C22B	−144.8 (2)
C16A—C11A—C21A—C26A	−36.7 (3)	C12B—C11B—C21B—C26B	−144.7 (2)
C12A—C11A—C21A—C26A	144.5 (2)	C16B—C11B—C21B—C26B	35.3 (3)
C26A—C21A—C22A—C23A	−1.5 (3)	C26B—C21B—C22B—C23B	1.3 (3)
C11A—C21A—C22A—C23A	178.9 (2)	C11B—C21B—C22B—C23B	−178.6 (2)

C21A—C22A—C23A—C24A	1.5 (3)	C21B—C22B—C23B—C24B	−0.5 (3)
C21A—C22A—C23A—C31A	−177.2 (2)	C21B—C22B—C23B—C31B	178.3 (2)
C22A—C23A—C24A—C25A	−0.5 (3)	C22B—C23B—C24B—C25B	−0.1 (3)
C31A—C23A—C24A—C25A	178.1 (2)	C31B—C23B—C24B—C25B	−178.8 (2)
C23A—C24A—C25A—C26A	−0.3 (4)	C23B—C24B—C25B—C26B	−0.1 (4)
C24A—C25A—C26A—C21A	0.2 (4)	C24B—C25B—C26B—C21B	0.9 (4)
C22A—C21A—C26A—C25A	0.7 (3)	C22B—C21B—C26B—C25B	−1.4 (3)
C11A—C21A—C26A—C25A	−179.8 (2)	C11B—C21B—C26B—C25B	178.4 (2)
C22A—C23A—C31A—C32A	32.0 (3)	C24B—C23B—C31B—C32B	145.9 (2)
C24A—C23A—C31A—C32A	−146.6 (2)	C22B—C23B—C31B—C32B	−32.8 (3)
C22A—C23A—C31A—C36A	−147.7 (2)	C24B—C23B—C31B—C36B	−36.0 (4)
C24A—C23A—C31A—C36A	33.7 (4)	C22B—C23B—C31B—C36B	145.3 (2)
C36A—C31A—C32A—C33A	2.2 (3)	C36B—C31B—C32B—C33B	−1.6 (3)
C23A—C31A—C32A—C33A	−177.5 (2)	C23B—C31B—C32B—C33B	176.6 (2)
C31A—C32A—C33A—C34A	−1.2 (3)	C31B—C32B—C33B—C34B	0.9 (3)
C31A—C32A—C33A—C41A	178.2 (2)	C31B—C32B—C33B—C41B	−177.8 (2)
C32A—C33A—C34A—C35A	−0.7 (3)	C32B—C33B—C34B—C35B	0.7 (4)
C41A—C33A—C34A—C35A	179.9 (2)	C41B—C33B—C34B—C35B	179.4 (2)
C33A—C34A—C35A—C36A	1.4 (4)	C33B—C34B—C35B—C36B	−1.6 (4)
C34A—C35A—C36A—C31A	−0.3 (4)	C34B—C35B—C36B—C31B	0.9 (4)
C32A—C31A—C36A—C35A	−1.5 (4)	C32B—C31B—C36B—C35B	0.7 (3)
C23A—C31A—C36A—C35A	178.2 (2)	C23B—C31B—C36B—C35B	−177.4 (2)
C32A—C33A—C41A—C46A	147.7 (2)	C32B—C33B—C41B—C42B	30.6 (3)
C34A—C33A—C41A—C46A	−32.9 (3)	C34B—C33B—C41B—C42B	−148.1 (2)
C32A—C33A—C41A—C42A	−31.6 (3)	C32B—C33B—C41B—C46B	−149.1 (2)
C34A—C33A—C41A—C42A	147.7 (2)	C34B—C33B—C41B—C46B	32.3 (3)
C46A—C41A—C42A—C43A	−0.2 (3)	C46B—C41B—C42B—C43B	0.2 (3)
C33A—C41A—C42A—C43A	179.2 (2)	C33B—C41B—C42B—C43B	−179.4 (2)
C41A—C42A—C43A—C44A	1.1 (3)	C41B—C42B—C43B—C44B	−0.5 (4)
C41A—C42A—C43A—C51A	−179.1 (2)	C41B—C42B—C43B—C51B	−179.1 (2)
C42A—C43A—C44A—C45A	−1.1 (3)	C42B—C43B—C44B—C45B	0.3 (4)
C51A—C43A—C44A—C45A	179.1 (2)	C51B—C43B—C44B—C45B	178.8 (2)
C43A—C44A—C45A—C46A	0.1 (4)	C43B—C44B—C45B—C46B	0.3 (4)
C44A—C45A—C46A—C41A	0.9 (4)	C44B—C45B—C46B—C41B	−0.6 (4)
C42A—C41A—C46A—C45A	−0.8 (4)	C42B—C41B—C46B—C45B	0.3 (4)
C33A—C41A—C46A—C45A	179.8 (2)	C33B—C41B—C46B—C45B	179.9 (2)
C44A—C43A—C51A—C56A	−34.2 (3)	C42B—C43B—C51B—C52B	35.9 (3)
C42A—C43A—C51A—C56A	146.1 (2)	C44B—C43B—C51B—C52B	−142.6 (3)
C44A—C43A—C51A—C52A	145.5 (2)	C42B—C43B—C51B—C56B	−143.4 (2)
C42A—C43A—C51A—C52A	−34.3 (3)	C44B—C43B—C51B—C56B	38.1 (3)
C56A—C51A—C52A—C53A	0.3 (4)	C56B—C51B—C52B—C53B	−1.6 (4)
C43A—C51A—C52A—C53A	−179.4 (2)	C43B—C51B—C52B—C53B	179.1 (2)
C51A—C52A—C53A—C54A	−0.1 (4)	C51B—C52B—C53B—C54B	0.6 (4)
C52A—C53A—C54A—C55A	0.2 (4)	C52B—C53B—C54B—C55B	0.5 (4)
C53A—C54A—C55A—C56A	−0.5 (4)	C53B—C54B—C55B—C56B	−0.4 (4)
C54A—C55A—C56A—C51A	0.7 (4)	C54B—C55B—C56B—C51B	−0.6 (4)
C52A—C51A—C56A—C55A	−0.5 (4)	C52B—C51B—C56B—C55B	1.6 (4)
C43A—C51A—C56A—C55A	179.1 (2)	C43B—C51B—C56B—C55B	−179.0 (2)

Dihedral angles (%) between adjacent planes

Rings	LT*A*	LT*B*	RT*A*	RT*B*
1–2	36.28 (11)	35.30 (12)	36.25 (9)	36.11 (9)
2–3	32.11 (11)	33.91 (11)	32.22 (8)	34.39 (8)
3–4	31.54 (11)	30.89 (12)	30.67 (8)	30.51 (9)
4–5	34.16 (12)	37.07 (13)	35.68 (10)	35.68 (10)

The angles are measured going from the ring containing atom C11 (ring 1) through to that containing C51 (ring 5) in all molecules.

MOLFIT parameters for overlays of all combinations of molecules from both polymorphs.

Molecule	Molecule	R.m.s. fit (wghtd) (Å)	Isometricity index (wghtd)	R.m.s. fit (unit weights) (Å)	Isometricity index (unit)	R.m.s. fit of bond lengths (Å)	R.m.s. fit of angles (°)	Fit Rotation Angle (°)
LT*A**	LT*B*	0.044	95.6	0.038	96.2	0.0045	0.297	179.68
RT*A**	RT*B*	0.053	94.7	0.049	95.1	0.0042	0.270	179.79
LT*A**	RT*A*	0.036	96.4	0.032	96.8	0.0065	0.353	89.91
LT*A*	RT*B*	0.063	93.7	0.060	94.0	0.0066	0.332	179.69
LT*B*	RT*A*	0.037	96.3	0.036	96.4	0.0072	0.316	-179.72
LT*B**	RT*B*	0.061	93.9	0.054	94.6	0.0076	0.292	-90.58

Note: * denotes an inverted molecule.

Coordinates of the centroids of the molecules in the asymmetric units of the LT and RT forms of (I).

Molecule	x	y	z	Δx	Δy	Δz
LT*A*	0.6876	0.7492	0.1196			
LT*B*	0.9459	0.2502	0.1187	0.2583	0.4990	0.0009
RT*A*	0.3231	0.1872	0.2602			
RT*B*	0.8220	0.4447	0.2655	0.4989	0.2575	0.0053

Short contacts between molecules

Polymorph	C	H	Ring (pivot atom)	Symmetry operator for ring	C—H	H···*Cg*	C···*Cg*	Angle at H
LT	C53B	H53B	*Cg*(C51A)	x, y, z	0.95	2.96	3.801 (3)	149
LT	C25B	H25B	*Cg*(C21A)	x + 1, y - 1, z	0.95	2.91	3.521 (3)	123
LT	C15A	H15A	*Cg*(C11B)	x - 1, y + 1, z	0.95	3.00	3.451 (3)	111
LT	C46A	H46A	*Cg*(C31B)	x, y, z	0.95	2.95	3.354 (2)	107
LT	C46B	H46B	*Cg*(C31A)	x, y - 1, z	0.95	3.00	3.319 (3)	101
RT	C53B	H53B	*Cg*(C51A)	x, y - 1, z	0.97	3.03	3.867	145
RT	C25B	H25B	*Cg*(C21A)	x + 1, y + 1, z	1.03	2.97	3.606	122
RT	C15A	H15A	*Cg*(C11B)	x - 1, y - 1, z	0.95	3.12	3.503	107
RT	C46A	H46A	*Cg*(C31B)	x, y, z	1.00	2.97	3.404	107
RT	C46B	H46B	*Cg*(C31A)	x + 1, y, z	0.99	3.06	3.346	98

Cg is the centre of gravity of the ring containing the indicated atom.